Integrated Passive-Active Model Identification with Tunable Model Discrimination for Affine Discrete-Time Systems

Changrui Liu, Qiang Shen, Ruochen Niu and Sze Zheng Yong

***Abstract*—This paper proposes a passive-active model identification algorithm for affine discrete-time systems that integrates active model discrimination (AMD) and model invalidation (MI). A look-up tree consisting of control inputs is constructed offline for this integrated model identification (IMI) technique to discriminate among models in a time-varying model set, which is only known at run time when repeatedly applying MI online. Furthermore, a novel tunable AMD (TAMD), with its mixed-integer linear programming (MILP) formulation, is proposed and combined with the IMI algorithm, which can improve model discrimination performance. The effectiveness of the proposed IMI algorithm is demonstrated through simulations for identifying intention models of human-driven vehicles in a lane changing scenario.**

***Index Terms*—Model Validation, Fault Diagnosis, Estimation**

I. Introduction

MODEL identification of system internal states (i.e., intention, fault or mode of operation) is an essential task for cyber-physical systems and is widely applicable to many engineering problems, e.g., achieving better collaboration among agents in networked control [1], detecting unknown malfunctions for safety critical systems [2], distinguishing the mode of operation for autonomous systems [3]. Thus, it is of great importance to develop model identification tools.

Literature Review: Model identification approaches have been well developed in the area of autonomous driving [3], smart building [4] and biochemical networks [5], and can be broadly categorized as passive and active methods. For traditional passive methods [4], [6], including MI, identification is achieved by passively utilizing the input-output sequence to falsify the unmatched models. Other extensions such as probabilistic MI [7] and MI using set-valued observer [8] have also been proposed. Unlike passive methods where inputs are not controlled, active methods design control inputs to actively influence the system behavior, which further assists the identification. One typical active method is AMD [3], [9], and its various variations, e.g., output feedback AMD [10], AMD with affine abstraction [11], multi-parametric AMD [12] and state-partitioned AMD [13]. Moreover, in [14], a closed-loop approach using a set-valued observer in a moving horizon framework is introduced. However, all these methods only ensure the separation between models at an unknown instance within the horizon, while when and how the models are separated fails to be well controlled. Another crucial issue is that, in practice, some models can be invalidated before the end of the time horizon if MI is applied at intermediate time steps, which reveals that current AMD techniques may generate inputs that are unnecessarily conservative for real applications since they implicitly assume that all models are possible candidates within the entire horizon.

Contributions: In contrast to passive methods that may fail to uniquely determine the true model and active methods that may apply overly conservative control inputs, we propose a more intelligent passive-active MI algorithm which solves the model identification task by probing the system with separating control inputs designed by AMD while continuously monitoring the valid models by MI at each time step. Since this integrated model identification (IMI) algorithm requires the AMD problem to discriminate among models in a time-varying model set which depends on the results of MI at run time, we propose an integrated algorithm that computes an IMI tree consisting of control inputs computed by AMD. This approach resembles the closed-loop AMD in [14] but involves MI instead of a conservative zonotope observer.

Moreover, to enable control of the separation index for each time segment of the time horizon, we propose a tunable AMD (TAMD) technique that allows weighting parameters in the optimization formulation of TAMD. TAMD improves on AMD by providing more design flexibility in terms of tunable separation indices to incorporate desired separation performance such as a preference for an early separation. In addition, TAMD is empirically found to result in significantly reduced computational time when compared to traditional AMD. Thus, this novel approach can benefit various applications such as active fault diagnosis and intent identification.

II. Preliminaries

A. Notation and Definitions

Let $x \in \mathbb{R}^n$ denote a vector with $x[k]$ and $\|x\|_i (i \in \{1, 2, \infty\})$ being its k-th element and vector norm. $M \in \mathbb{R}^{n\times m}$ is a matrix with $M^\top$, $M[:,k]$ and $M[k,:]$ being its transpose, k-th column and k-th row, respectively. $M \geq 0$

Manuscript received Sept. 14, 2021; revised Nov. 24, 2021; accepted Dec. 3, 2021. This work was supported in part by the Natural Science Foundation of China under Grant 62103275 and National Science Foundation Grant CNS-1943545.

C. Liu is with the Department of Control and Simulation, Faculty of Aerospace Engineering, Delft University of Technology, Delft, The Netherlands (e-mail: C.Liu-31@student.tudelft.nl, lcrekko@gmail.com).

Q. Shen is with the School of Aeronautics and Astronautics, Shanghai Jiao Tong University, Shanghai, P.R. China (e-mail: qiangshen@sjtu.edu.cn).

R. Niu and S. Z. Yong are with the School for Engineering of Matter, Transport and Energy, Arizona State University, Tempe, AZ, USA (e-mail:{rniu6, szyong}@asu.edu).

Digital Object Identifier

$(x \geq 0)$ denote element-wise non-negativity. $\mathbf{0}$, $\mathbb{1}$ and $\mathbb{I}$ are zero vector, one vector and identity matrix, respectively. The set of positive integers up to n is $\mathbb{Z}_n^+$, and $\mathbb{Z}_j^i$ denotes non-negative integers from i to j $(0 \leq i \leq j)$. Further, we define operators diag and vec for matrices (vectors) as:

$$\text{diag}_N\{M_i\} = \mathbb{I}_N \otimes M_i \ , \quad \text{vec}_N\{M_i\} = \mathbb{1}_N \otimes M_i \ ,$$

$$\text{diag}_{i,j}\{M_k\} = \begin{bmatrix} M_i & \mathbf{0} \\ \mathbf{0} & M_j \end{bmatrix}, \quad \text{vec}_{i,j}\{M_k\} = \begin{bmatrix} M_i \\ M_j \end{bmatrix},$$

$$\text{diag}_{k=i}^{j}\{M_k\} = \begin{bmatrix} M_i & & \\ & \ddots & \\ & & M_j \end{bmatrix}, \quad \text{vec}_{k=i}^{j}\{M_k\} = \begin{bmatrix} M_i \\ \vdots \\ M_j \end{bmatrix},$$

where $i, j \in \mathbb{Z}_n^+$ and $\otimes$ is the Kronecker product.

Definition 1 (Linear Partition)**.** *A linear partition of integer set $\mathbb{Z}_j^i$ is a collection of ℓ disjoint integer subsets $\mathbb{Z}_{\overline{\tau}}^{\underline{\tau}}$ $(\tau \in \mathbb{Z}_\ell^+)$ for any $\underline{\tau}, \overline{\tau}$ that satisfy $i := \underline{1} \leq \overline{1}, \overline{1}{+}1 =: \underline{2} \leq \overline{2}, \ldots, \overline{l-1}+1 =: \underline{l} \leq \overline{l} := j$. The linear partition is complete if $\ell = j{-}i{+}1$.*

Definition 2 (Reduced Power Set (RPS))**.** *Given a set $\mathcal{S}$ with its power set $2^{\mathcal{S}}$, its RPS is defined as $2_{re}^{\mathcal{S}} := \{\mathcal{S}_i \in 2^{\mathcal{S}} : |\mathcal{S}_i| \geq 2\}$. The RPS of $\mathbb{Z}_n^+$ is denoted as 2_{re}^n.*

B. Modeling Framework

Consider systems with N distinct models, each model $\mathcal{G}_i$ is a discrete-time affine time-invariant process as:

$$\bar{\boldsymbol{x}}_i(k+1) = A_i\bar{\boldsymbol{x}}_i(k) + [B_{u,i}, B_{d,i}]\bar{\boldsymbol{u}}_i(k) + B_{w,i}w_i(k) + f_i, \quad (1)$$

$$z_i(k) = C_i\bar{\boldsymbol{x}}_i(k) + D_{v,i}v_i(k) + g_i. \quad (2)$$

where $\bar{\boldsymbol{x}}_i \in \mathbb{R}^n$ is the states, $\bar{\boldsymbol{u}}_i \in \mathbb{R}^m$ is the inputs, $z_i \in \mathbb{R}^{n_z}$ is the outputs, $w_i \in \mathbb{R}^{m_w}$ and $v_i \in \mathbb{R}^{m_v}$ are the process noise and the measurement noise, respectively.

The initial condition of model i, denoted by $\bar{\boldsymbol{x}}_i^0 = \bar{\boldsymbol{x}}_i(0)$, is constrained to a polyhedral set with c_0 inequalities:

$$\bar{\boldsymbol{x}}_i^0 \in \mathcal{X}_0 = \{\bar{\boldsymbol{x}} \in \mathbb{R}^n : P_0\bar{\boldsymbol{x}} \leq p_0\}, \ \forall i \in \mathbb{Z}_N^+. \quad (3)$$

The inputs consists of controllable inputs $u \in \mathbb{R}^{m_u}$ and model-dependent uncontrolled disturbances $d_i \in \mathbb{R}^{m_d}$. At any time instant k, the controls and disturbances are also constrained to polyhedral sets with c_u and c_d inequalities:

$$u(k) \in \mathcal{U} = \{u \in \mathbb{R}^{m_u} : Q_u u \leq q_u\}, \quad (4)$$

$$d_i(k) \in \mathcal{D}_i = \{d \in \mathbb{R}^{m_d} : Q_{d,i}d \leq q_{d,i}\}. \quad (5)$$

Subsequently, the states are also divided as $\bar{\boldsymbol{x}}_i = [x_i^\top, y_i^\top]^\top$, where $x_i \in \mathbb{R}^{n_x}$ denotes the controlled states that are associated with u and $y_i \in \mathbb{R}^{n_y}$ denotes uncontrolled states that are only perturbed by d_i. Both the controlled and uncontrolled states need to satisfy, respectively, their corresponding polyhedral constraints with c_x and c_y inequalities:

$$x_i(k) \in \mathcal{X}_{x,i} = \{x \in \mathbb{R}^{n_x} : P_{x,i}x \leq p_{x,i}\}, \quad (6)$$

$$y_i(k) \in \mathcal{X}_{y,i} = \{y \in \mathbb{R}^{n_y} : P_{y,i}y \leq p_{y,i}\}. \quad (7)$$

The process and measurement noise w_i, v_i are also polyhedrally constrained with c_w and c_v inequalities, respectively:

$$w_i(k) \in \mathcal{W}_i = \{w \in \mathbb{R}^{m_w} : Q_{w,i}w \leq q_{w,i}\}, \quad (8)$$

$$v_i(k) \in \mathcal{V}_i = \{v \in \mathbb{R}^{m_v} : Q_{v,i}v \leq q_{v,i}\}. \quad (9)$$

C. Time & Pair Concatenation

Given time horizon T, we first introduce time-concatenated notation for variables of model i as follows:

$$\bullet_{i,t}^{+} = \text{vec}_{k=1}^{t}\{\bullet_i(k)\}, \quad \bullet_{i,t} = \text{vec}_{k=0}^{t}\{\bullet_i(k)\},$$

where $\bullet \in \{\bar{\boldsymbol{x}}, x, y, d, w, v, z\}$ and $t \in \mathbb{Z}_T^+$. Next, with N models, there are $I = \binom{N}{2}$ model pairs in total and let $\nu \in \mathbb{Z}_I^+$ denote the pair index for model pair (i, j). Then, we construct pair-concatenated notations as follows:

$$\bullet_{\nu,t}^{+} = \text{vec}_{i,j}\{\bullet_{k,t}^{+}\}, \quad \bullet_{\nu,t} = \text{vec}_{i,j}\{\bullet_{k,t}\},$$

as well as pair-concatenated initial states $\bar{\boldsymbol{x}}_\nu^0 = \text{vec}_{i,j}\{\bar{\boldsymbol{x}}_k^0\}$ and time-concatenated controls $u_t = \text{vec}_{k=0}^{t}\{u(k)\}$.

Likewise, all the matrices and vectors in from (5) to (9) are first time-concatenated as follows:

$$\bar{P}_{\diamond,i}^t = \text{diag}_t\{P_{\diamond,i}\}, \quad \bar{Q}_{\star,i}^t = \text{diag}_t\{Q_{\star,i}\},$$

$$\bar{p}_{\diamond,i}^t = \text{vec}_t\{p_{\diamond,i}\}, \quad \bar{q}_{\star,i}^t = \text{vec}_t\{q_{\star,i}\},$$

where $\diamond \in \{x, y\}$ and $\star \in \{d, w, v\}$.

Then, pair-concatenation follows directly as follows:

$$\bar{P}_{\diamond,\nu}^t = \text{diag}_{i,j}\{\bar{P}_{\diamond,k}^t\}, \quad \bar{Q}_{\star,\nu}^t = \text{diag}_{i,j}\{\bar{Q}_{\star,k}^t\},$$

$$\bar{p}_{\diamond,\nu}^t = \text{vec}_{i,j}\{\bar{p}_{\diamond,k}^t\}, \quad \bar{q}_{\star,\nu}^t = \text{vec}_{i,j}\{\bar{q}_{\star,k}^t\}.$$

For the constraints in (4), we consider time-concatenation $\bar{Q}_u^t = \text{diag}_t\{Q_u\}$ and $\bar{q}_u^t = \text{vec}_t\{q_u\}$, while for constraints on the initial states in (3), only trivial concatenation $\bar{P}_0 = \text{diag}_2\{P_0\}$ and $\bar{p}_0 = \text{vec}_2\{p_0\}$ are required.

Based on the model dynamics (1) and (2), we can obtain the time-concatenated dynamics for $t \in \mathbb{Z}_T^+$ as follows:

$$\bar{\boldsymbol{x}}_{i,t}^{+} = M_i^t\bar{\boldsymbol{x}}_i^0 + \Omega_{ui}^t u_{t-1} + \Gamma_{di}^t d_{i,t-1} + \Gamma_{wi}^t w_{i,t-1} + \bar{f}_i^t, \quad (10)$$

$$x_{i,t}^{+} = M_i^{x,t}\bar{\boldsymbol{x}}_i^0 + \Omega_{ui}^{x,t}u_{t-1} + \Gamma_{di}^{x,t}d_{i,t-1} + \Gamma_{wi}^{x,t}w_{i,t-1} + \bar{f}_i^{x,t}, \quad (11)$$

$$y_{i,t}^{+} = M_i^{y,t}\bar{\boldsymbol{x}}_i^0 + \Omega_{ui}^{y,t}u_{t-1} + \Gamma_{di}^{y,t}d_{i,t-1} + \Gamma_{wi}^{y,t}w_{i,t-1} + \bar{f}_i^{y,t}, \quad (12)$$

$$z_{i,t}^{+} = \bar{C}_i^t\bar{\boldsymbol{x}}_i^0 + \bar{E}_{ui}^t u_{t-1} + \bar{D}_{di}^t d_{i,t-1} + \bar{D}_{wi}^t w_{i,t-1} + \bar{D}_{vi}^t v_{i,t}^{+} + \bar{\theta}_i^t. \quad (13)$$

The matrices of pair-concatenated dynamics can simply be built upon the matrices and vectors in from (10) to (13) given in the Appendix. For pair $\nu = (i, j)$, the following holds:

$$\S_{(\star)\nu}^{(\diamond),t} = \text{diag}\{\S_{(\star)i}^{(\diamond),t}, \S_{(\star)j}^{(\diamond),t}\}, \quad \ddagger_{(u)\nu}^{(\diamond),t} = \text{vec}\{\ddagger_{(u)i}^{(\diamond),t}, \ddagger_{(u)j}^{(\diamond),t}\},$$

where $\S \in \{M, \Gamma, \bar{C}, \bar{D}\}$ and $\ddagger \in \{\Omega, \bar{E}, \bar{f}, \bar{\theta}\}$.

Moreover, the uncertain variable for model i is defined as $\bar{x}_{i,t} = \text{vec}\{\bar{\boldsymbol{x}}_i^0, d_{i,t-1}, w_{i,t-1}, v_{i,t}^{+}\}$. Similarly, for model pair ν, we have $\bar{x}_{\nu,t} = \text{vec}\{\bar{\boldsymbol{x}}_\nu^0, d_{\nu,t-1}, w_{\nu,t-1}, v_{\nu,t}^{+}\}$. Correspondingly, we form $H_{\bar{x},i}^t = \text{diag}\{P_0, \bar{Q}_{d,i}^t, \bar{Q}_{w,i}^t, \bar{Q}_{v,i}^t\}$, $h_{\bar{x},i}^t = \text{vec}\{p_0, \bar{q}_{d,i}^t, \bar{q}_{w,i}^t, \bar{q}_{v,i}^t\}$ for $\bar{x}_{i,t}$ such that $H_{\bar{x},i}^t\bar{x}_{i,t} \leq h_{\bar{x},i}^t$ follows as combined model uncertainty constraints. Also, for $\bar{x}_{\nu,t}$, we build $H_{\bar{x},\nu}^t = \text{diag}\{\bar{P}_0, \bar{Q}_{d,\nu}^t, \bar{Q}_{w,\nu}^t, \bar{Q}_{v,\nu}^t\}$ and $h_{\bar{x},\nu}^t = \text{vec}\{\bar{p}_0, \bar{q}_{d,\nu}^t, \bar{q}_{w,\nu}^t, \bar{q}_{v,\nu}^t\}$ such that pair uncertainty constraints $H_{\bar{x},\nu}^t\bar{x}_{\nu,t} \leq h_{\bar{x},\nu}^t$ is established.

Finally, we can rewrite time-concatenated dynamics in terms of the uncertain variable as follows:

$$\bar{\boldsymbol{x}}_{i,t}^{+} = \Phi_i^t\bar{x}_{i,t} + \Omega_{ui}^t u_{t-1} + \bar{f}_i^t, \quad (14a)$$

$$x_{i,t}^{+} = \Phi_i^{x,t}\bar{x}_{i,t} + \Omega_{ui}^{x,t}u_{t-1} + \bar{f}_i^{x,t}, \quad (14b)$$

$$y_{i,t}^{+} = \Phi_i^{y,t}\bar{x}_{i,t} + \Omega_{ui}^{y,t}u_{t-1} + \bar{f}_i^{y,t}, \quad (14c)$$

$$z_{i,t}^{+} = \Psi_i^t\bar{x}_{i,t} + \bar{E}_{ui}^t u_{t-1} + \bar{\theta}_i^t, \quad (14d)$$

and pair-concatenated dynamics similarly as follows:

$$y_{\nu,t}^{+} = \Phi_\nu^{y,t}\bar{x}_{\nu,t} + \Omega_{u\nu}^{y,t}u_{t-1} + \bar{f}_\nu^{y,t} \ , \quad (15a)$$

$$z_{\nu,t}^{+} = \Psi_\nu^t\bar{x}_{\nu,t} + \bar{E}_{u\nu}^t u_{t-1} + \bar{\theta}_\nu^t \ , \quad (15b)$$

where in (14), $\Phi_i^{(\diamond),t} = [M_i^{(\diamond),t}, \Gamma_{di}^{(\diamond),t}, \Gamma_{wi}^{(\diamond),t}, \mathbf{0}]$, $\Psi_i^t = [\bar{C}_i^t, \bar{D}_{di}^t, \bar{D}_{wi}^t, \bar{D}_{vi}^t]$, and in (15), $\Phi_\nu^{y,t} = [M_\nu^{y,t}, \Gamma_{d\nu}^{y,t}, \Gamma_{w\nu}^{y,t}, \mathbf{0}]$, $\Psi_\nu^t = [\bar{C}_\nu^t, \bar{D}_{d\nu}^t, \bar{D}_{w\nu}^t, \bar{D}_{v\nu}^t]$.

III. Problem Formulation

In this section, detailed formulations of the TAMD, online MI and IMI tree construction will be given.

A. Tunable Active Model Discrimination (TAMD)

The function of TAMD is twofold. First, it designs a separating input which, if being applied, makes the reachable output set of any pair of models have no intersection (i.e., completely separated) for at least one time instant within time horizon T, taking all possible realizations of uncertainty into account. Second, the extent to which the models are separated and when the complete separation is enforced are controlled by tuning the weights in the TAMD formulation.

Consider a linear partition of $\mathbb{Z}_T^0$ that results in $\mathbb{Z}_{\underline{\tau}}^{\overline{\tau}} (\tau \in \mathbb{Z}_\ell^+)$ segments. For each segment τ, the output trajectories of any pair of models have to differ by a threshold $\epsilon_\tau - s_\tau$ for at least one instant, where ϵ_τ is the preset desired separation and s_τ denotes the soft variable describing the violation of the desired separation. Also, we introduce binary variables a_τ such that $a_\tau = 1$ implies $s_\tau \leq 0$, which leads to

$$s_\tau \leq M(1 - a_\tau),\ \forall \tau \in \mathbb{Z}_\ell^+ \tag{16}$$

where M is a big constant. To achieve desired separation for at least one segment starting from segment κ, we have

$$\sum\nolimits_{\tau=\kappa}^{\ell} a_\tau \geq 1 \tag{17}$$

Subsequently, the problem of TAMD is formally defined as:

Problem 1 (Tunable Active Model Discrimination)**.** *Given a system consisting of N well-posed [3] affine models $\mathcal{G}_i$, a linear partition of $\mathbb{Z}_T^+$ with preset desired separation $\epsilon_\tau (\tau \in \mathbb{Z}_\ell^+)$, the set of indices of remaining possible valid models $\mathbb{V}_t \in 2_{re}^N$ at time instant $t \in \mathbb{Z}_{T-1}^0$ with t belonging to the κth segment of the partition, and fixed control inputs from 0 to $t-1$ denoted as u_{t-1}^*, design an optimal control inputs u_{T-1}, such that for all possible initial states $\bar{\boldsymbol{x}}_i^0$, uncontrolled inputs $d_{i,T-1}$, process noise $w_{i,T-1}$, measurement noise $v_{i,T}^+$, and for all $\kappa \leq \tau \leq \ell$, the output trajectories starting from $t+1$ of any pair of models in $\mathbb{V}_t$ have to differ by a threshold $\epsilon_\tau - s_\tau$ in at least one time instance within time segment τ. This problem is mathematically stated as follows:*

$$u_{T-1}^* = \underset{u_{T-1}, s_\tau}{\arg\min}\ J(u_{T-1}) + \sum\nolimits_{\tau=\kappa}^{\ell} \lambda_\tau s_\tau$$

$$\textit{s.t.}\quad \forall k \in \mathbb{Z}_{T-1}^t : (4)\ \textit{holds}, \tag{18a}$$

$$\forall k \in \mathbb{Z}_{t-1}^0 : u_{T-1}(k) = u_{t-1}^*(k), \tag{18b}$$

$$\forall \tau \in \mathbb{Z}_\ell^\kappa : (16),\ (17)\ \textit{hold}, \tag{18c}$$

$$\left.\begin{array}{r} \forall i \in \mathbb{V}_t, \\ \forall \bar{\boldsymbol{x}}_i^0 \in \mathcal{X}_0, \forall k \in \mathbb{Z}_{T-1}^0, \\ \forall y_i(k+1), d_i(k), \\ \forall w_i(k), v_i(k+1) : \\ (1)\text{-}(3),\ (5),\ (7)\text{-}(9)\ \textit{hold}; \end{array}\right\} : \begin{array}{l} \{\forall k \in \mathbb{Z}_T^+ : (6)\ \textit{holds}\} \wedge \\ \{\forall i, j \in \mathbb{V}_t, i \neq j, \\ \forall \tau \in \mathbb{Z}_\ell^\kappa, \\ \exists k_\tau^* \in \mathbb{Z}_{\underline{\tau}}^{\overline{\tau}}, k_\tau^* \geq t+1 : \\ |z_i(k_\tau^*) - z_j(k_\tau^*)| \geq \\ \qquad (\epsilon_\tau - s_\tau)\mathbb{1}\}, \end{array} \tag{18d}$$

where $J(\cdot)$ is the objective for the control inputs and λ_τ are constant weights for penalizing the soft variables s_τ.

Remark 1. *Tuning the weights λ_τ enables control over the desired separation at the design stage. Choosing a large value for λ_τ enforces a larger separation for segment τ.*

Remark 2. *The fixed control u_{t-1}^* satisfies (4) by assumption or by the design of the IMI tree in Algorithm 1. Besides, when $t = 0$, u_{-1}^* does not exist and (18b) can be ignored.*

B. Model Invalidation (MI)

Before formally stating the model invalidation problem, we give the definition of model behavior similar to [15].

Definition 3 (t-truncated Model Behavior)**.** *The t-truncated model behavior of model $\mathcal{G}_i$ is the set of all admissible input-output trajectories of length t, given by the set*

$$\begin{aligned} \mathcal{B}^t(\mathcal{G}_i) := \big\{ & \{u(k), z(k+1)\}_{k=0}^{t-1} :\ u(k) \in \mathcal{U}\ \textit{and} \\ & \exists \bar{\boldsymbol{x}}_i(k+1) \in \mathcal{X}_i, \bar{\boldsymbol{x}}_i^0 \in \mathcal{X}_0, d_i(k) \in \mathcal{D}_i, w_i(k) \in \mathcal{W}_i, \\ & v_i(k+1) \in \mathcal{V}_i, \forall k \in \mathbb{Z}_{t-1}^0\ \textit{s.t.}\ (1), (2)\ \textit{hold}\ \big\} \end{aligned}$$

Then, we formally define the problem of model invalidation in terms of the model behavior set $\mathcal{B}^t(\mathcal{G}_i)$ as follows:

Problem 2 (Model Invalidation)**.** *Given model $\mathcal{G}_i$, all constraints given in from (3) to (9) and input-output sequence $\{\tilde{u}(k), \tilde{z}(k+1)\}_{k=0}^{t-1}$, determine whether or not this sequence belongs to the behavior set $\mathcal{B}^t(\mathcal{G}_i)$. This problem is equivalent to checking the feasibility of the following problem:*

$$\begin{aligned} & \textit{Find}\ \bar{\boldsymbol{x}}_i(k+1), \bar{\boldsymbol{x}}_i^0, d_i(k), w_i(k), v_i(k+1), \forall k \in \mathbb{Z}_{t-1}^0 \\ & \textit{s.t.}\ (1)\text{–}(3), (5)\text{–}(9)\ \textit{hold},\ \forall k \in \mathbb{Z}_{t-1}^0. \end{aligned} \tag{19}$$

Having formulated the MI problem, we can further state the online model selection problem that is built upon MI.

Problem 3 (Online Model Selection)**.** *Given the set of index of possible valid models $\mathbb{V}_t \in 2_{re}^n$ at time $t \in \mathbb{Z}_{T-1}^0$, models $\mathcal{G}_i, \forall i \in \mathbb{V}_t$, the input-output sequence $\{\tilde{u}(k), \tilde{z}(k+1)\}_{k=0}^{t-1}$ up to time instant $t-1$, and the newly applied control $\tilde{u}(t)$ with output $\tilde{z}(t+1)$, compute valid models $\mathbb{V}_{t+1}$ at step $t+1$.*

Remark 3. *Solving the online model selection involves applying MI to each candidate model in parallel to rule out the invalid models using $\tilde{u}(t)$ designed by TAMD offline and extracted from the look-up tree (cf. Problem 4). Further, at step 0, we have $\{\tilde{u}(k), \tilde{z}(k+1)\}_{k=0}^{-1} = \emptyset$ and $\mathbb{V}_0 = \mathbb{Z}_N^+$.*

Remark 4. *The final IMI problem involves recursively solving the online model selection problem starting from $t = 0$.*

C. Integrated Model Identification Tree (IMI Tree)

To formulate the problem of building the IMI tree, it is essential to express how the set of possible valid models is updated. Based on $\mathbb{V}_t$, a sequence of $\mathbb{V}_t$ forms a trace ω, then all traces form a tree $\mathcal{T}$. Formal definitions of these concepts are given as follows:

Definition 4 (Normal Trace & Identical Trace)**.** *Given time horizon T, time interval $[\underline{t}, \bar{t}]$ and $\mathbb{V}_{\underline{t}}$ at time $\underline{t}$, the corresponding length $\bar{t} - \underline{t} + 1$ normal trace, denoted as $\omega_{\bar{t}}(\mathbb{V}_{\underline{t}})$, is a sequence of index set $\{\mathbb{V}_k\}_{k=\underline{t}}^{\bar{t}} (\mathbb{V}_k \in 2_{re}^N)$ such that $\mathbb{V}_k \supseteq \mathbb{V}_{k+1}$. A trace is called an identical trace if $\mathbb{V}_k = \mathbb{V}_{k+1}, \forall k \in [\underline{t}, \bar{t}]$, and is denoted as $\omega_{\bar{t}}^*(\mathbb{V}_{\underline{t}})$. The element of any trace at k is denoted as $\omega_{\bar{t}}(\mathbb{V}_{\underline{t}})[k]$ $(k \in \mathbb{Z}_{\bar{t}}^{\underline{t}})$.*

Definition 5 (Branch)**.** *The branch $\mathcal{BR}_{\bar{t}}(\omega_\alpha(\mathbb{V}_{\underline{t}}))$ is the set of all traces whose first $\alpha - \underline{t} + 1$ entries are the same as $\omega_\alpha(\mathbb{V}_{\underline{t}})$, formally expressed as*

$$\begin{aligned} \mathcal{BR}_{\bar{t}}(\omega_\alpha(\mathbb{V}_{\underline{t}})) := \big\{ & \{\mathbb{V}_k\}_{k=\underline{t}}^{\bar{t}} : \mathbb{V}_k \in 2_{re}^N, \mathbb{V}_k \supseteq \mathbb{V}_{k+1}, \\ & \forall k \in \mathbb{Z}_\alpha^{\underline{t}}, \mathbb{V}_k = \omega_\alpha(\mathbb{V}_{\underline{t}})[k] \big\}. \end{aligned}$$

Definition 6 (Tree)**.** *The tree $\mathcal{T}_{\bar{t}}^{\underline{t}}(\mathbb{V}_{\underline{t}})$ is the set of all traces $\omega_{\bar{t}}(\mathbb{V}_{\underline{t}})$, formally expressed as*

$$\mathcal{T}_{\bar{t}}^{\underline{t}}(\mathbb{V}_{\underline{t}}) := \big\{ \{\mathbb{V}_k\}_{k=\underline{t}}^{\bar{t}} : \mathbb{V}_k \in 2_{re}^N, \mathbb{V}_k \supseteq \mathbb{V}_{k+1} \big\}.$$

Then, the problem of computing inputs for the tree is formally given as:

Problem 4 (Construction of IMI Tree)**.** *Given time horizon T and N models $\mathcal{G}_i$, for each trace in the tree $\mathcal{T}^0_{T-1}(\mathbb{Z}^+_N)$, design an optimal separating control input by TAMD.*

IV. Main Approaches

In this section, we first provide an MILP formulation of TAMD and an IMI tree construction algorithm. Then, we provide an LP formulation for MI, followed by the final IMI.

A. Tunable Active Model Discrimination

TAMD can be posed as an bilevel optimization problem, which then is reformulated as a single level MILP by applying KKT conditions to the inner problems. The bilevel formulation is given by the following lemma:

Lemma 1 (Bilevel Formulation of TAMD)**.** *Given linear partition $\mathbb{Z}^{\overline{\tau}}_{\underline{\tau}}$ of $\mathbb{Z}^+_T$, the index set $\mathbb{V}_t$ ($N_t := |\mathbb{V}_t|$) with the number of pairs $I_t = \binom{N_t}{2}$, TAMD in Problem 1 is equivalent to a bilevel optimization whose outer problem is given as:*

$$u^*_{T-1} = \arg\min_{u_{T-1}, s_\tau} J(u_{T-1}) + \textstyle\sum_{\tau=\kappa}^{\ell} \lambda_\tau s_\tau \qquad (\text{P}_{\text{Outer}})$$

$$\text{s.t.} \quad \forall k \in \mathbb{Z}^t_{T-1} : (4) \textit{ holds}, \qquad (20a)$$

$$\forall k \in \mathbb{Z}^0_{t-1} : u_{T-1}(k) = u^*_{t-1}(k), \qquad (20b)$$

$$\left.\begin{array}{r}\forall i \in \mathbb{V}_t, \forall \bar{\boldsymbol{x}}^0_i \in \mathcal{X}_0, \forall k \in \mathbb{Z}^0_{T-1},\\ \forall y_i(k+1), d_i(k),\\ \forall w_i(k), v_i(k+1):\\ (1)\text{-}(3),\ (5),\ (7)\text{-}(9)\ \textit{hold}\end{array}\right\} : \forall k \in \mathbb{Z}^+_T : (6) \textit{ holds}, \qquad (20c)$$

$$\forall \tau \in \mathbb{Z}^\kappa_\ell, \forall \nu \in \mathbb{Z}^+_{I_t} : \delta^*_{\nu,\tau} \geq \epsilon_\tau - s_\tau, \qquad (20d)$$

$$(16),\ (17)\ \textit{hold}, \qquad (20e)$$

where $\delta^*_{\nu,\tau}$ is the optimal solution of the following inner problem for pair ν and segment τ

$$\delta^*_{\nu,\tau}(u^t_{\overline{\tau}-1}) = \min_{\delta_{\nu,\tau}, \bar{\boldsymbol{x}}^0_\nu, d_{\nu,\overline{\tau}-1}, w_{\nu,\overline{\tau}-1}, v^+_{\nu,\overline{\tau}-1}} \delta_{\nu,\tau} \qquad (\text{P}_{\text{inner}}(\nu,\tau))$$

$$\text{s.t.} \quad \textit{for } \nu = (i,j):$$

$$\begin{cases} \forall k \in \mathbb{Z}_{\overline{\tau}-1}: \ (1) \textit{ holds},\\ \forall k \in \mathbb{Z}^+_{\overline{\tau}}: \ (2) \textit{ holds},\\ \forall k \in \mathbb{Z}^{\overline{\tau}}_{\underline{\tau}}, k \geq t+1: \ |z_i(k) - z_j(k)| \leq \delta_{\nu,\tau}\mathbb{1},\\ \forall\, \bar{\boldsymbol{x}}^0_\nu, d_{\nu,\overline{\tau}-1}, w_{\nu,\overline{\tau}-1}, v^+_{\nu,\overline{\tau}-1}: \ (3), (5), (7)\text{–}(9)\ \textit{hold}. \end{cases} \qquad (21a)$$

Proof. The proof follows a similar procedure as in [3]. □

Then, employing robust optimization to the outer problem and KKT conditions to the inner problems, we obtain the final single level MILP in the following theorem:

Theorem 1. *Suppose $\bar{P}^T_{y,i}\Omega^{y,T}_{ui} = 0$. The bilevel optimization problem in Lemma 1 is equivalent to a MILP as:*

$$u^*_{T-1} = \arg\min_{u_{T-1}, s_\tau, \bar{x}_{\nu,T}, \boldsymbol{\Pi}_i, \boldsymbol{\mu}^1_{\nu\tau}, \boldsymbol{\mu}^2_{\nu\tau}} J(u_{T-1}) + \textstyle\sum_{\tau=\kappa}^{\ell} \lambda_\tau s_\tau$$

$$\text{s.t.} \quad \bar{Q}^{T-t}_u u^t_{T-1} \leq \bar{q}^{T-t}_u, \qquad (22a)$$

$$\forall k \in \mathbb{Z}^0_{t-1} : u_{T-1}(k) = u^*_{t-1}(k), \qquad (22b)$$

$$\forall i \in \mathbb{V}_t : \boldsymbol{\Pi}_i \geq 0, \boldsymbol{\Pi}_i^\top \begin{bmatrix} H^T_{\bar{x},i} \\ \bar{P}^T_{y,i}\Phi^{y,T}_i \end{bmatrix} = \bar{P}^T_{x,i}\Phi^{x,T}_i, \qquad (22c)$$

$$\boldsymbol{\Pi}_i^\top \begin{bmatrix} h^T_{\bar{x},i} \\ \bar{p}^T_{y,i} - \bar{P}^T_{y,i}\bar{f}^{y,T}_i \end{bmatrix} \leq \begin{array}{c} \bar{p}^T_{x,i} - \bar{P}^T_{x,i}\bar{f}^{x,T}_i \\ -(\bar{P}^T_{x,i}\Omega^{x,T}_{ui})u_{T-1}, \end{array} \qquad (22d)$$

$$\forall \tau \in \mathbb{Z}^\kappa_\ell, \forall \nu \in \mathbb{Z}^+_{I_t} : \delta_{\nu,\tau}(u_{\overline{\tau}-1}) \geq \epsilon_\tau - s_\tau, \qquad (22e)$$

$$(16), (17), (23), (24)\ \textit{hold}, \qquad (22f)$$

where details of the dual variables $\boldsymbol{\Pi}_i$, $\boldsymbol{\mu}^1_{\nu\tau}$, $\boldsymbol{\mu}^2_{\nu\tau}$, and constraints (23), (24) are provided in the proof.

Proof. First, (22a) is the concatenated form of (20a), and (22b) is exactly the same as (20b).

Next, due to $\bar{P}^T_{y,i}\Omega^{y,T}_{ui} = 0$, the responsibility of the uncontrolled states is not influenced by u_{T-1}. Consequently, constraints (20c) is reformulated as its robust counterpart given in (22c) and (22d) using dual matrix variable $\boldsymbol{\Pi}_i$.

Before applying KKT conditions to the inner problems, we rewrite the output difference constraints in a compact form:

$$(\Xi_{\overline{\tau}}\Psi^{\overline{\tau}}_\nu)\bar{x}_{\nu,\overline{\tau}} \leq \delta_{\nu,\tau}\mathbb{1} - (\Xi_{\overline{\tau}}\bar{E}^{\overline{\tau}}_{u\nu})u_{\overline{\tau}-1} - \Xi_{\overline{\tau}}\theta^{\overline{\tau}}_\nu$$

where $\Xi_{\overline{\tau}} = [\mathbb{I}, -\mathbb{I}; -\mathbb{I}, \mathbb{I}]$ with $\mathbb{I}$ of dimension $p\overline{\tau}$. Let $t_s = max\{\underline{\tau}, t+1\}$, from the above inequality, we extract the rows from pt_s to $p\overline{\tau}$ and from $2pt_s$ to $2p\overline{\tau}$, then append these $2p(\overline{\tau} - t_s + 1)$ rows to build the following:

$$\Lambda_{\nu,\tau}\bar{x}_{\nu,\overline{\tau}} \leq \delta_{\nu,\tau}\mathbb{1} - L_{\nu,\tau}u_{\overline{\tau}-1} - b_{\nu,\tau}.$$

Then, the separability constraints in (21a) can be written as

$$\begin{bmatrix} H^{\overline{\tau}}_{\bar{x},\nu} \\ \bar{P}^{\overline{\tau}}_{y,\nu}\Phi^{y,\overline{\tau}}_\nu \\ \Lambda_{\nu,\tau} \end{bmatrix} \bar{x}_{\nu,\overline{\tau}} \leq \delta_{\nu,\tau} \begin{bmatrix} \mathbf{0} \\ \mathbf{0} \\ \mathbb{1} \end{bmatrix} - \begin{bmatrix} \mathbf{0} \\ \mathbf{0} \\ L_{\nu,\tau} \end{bmatrix} u_{\overline{\tau}-1} + \begin{bmatrix} h^{\overline{\tau}}_{\bar{x},\nu} \\ \bar{P}^{\overline{\tau}}_{y,\nu}\bar{f}^{y,\overline{\tau}}_\nu \\ -b_{\nu,\tau} \end{bmatrix}$$

and for convenience, we denote the above inequality as

$$R_{\nu,\tau}\bar{x}_{\nu,\overline{\tau}} \leq \delta_{\nu,\tau} \begin{bmatrix} \mathbf{0} \\ \mathbf{0} \\ \mathbb{1} \end{bmatrix} - S_{\nu,\tau}u_{\overline{\tau}-1} + r_{\nu,\tau}. \qquad (23)$$

In (23), the number of columns of $R_{\nu,\tau}$ is $\xi = 2(n + \overline{\tau}m_s)$ with $m_s = m_d + m_w + m_v$. To apply KKT conditions, we introduce the dual variables $\boldsymbol{\mu}^1_{\nu\tau}[i](i \in \mathbb{Z}^+_\rho)$ for the first $\rho = 2(c_0 + \overline{\tau}c_s)$ rows with $c_s = c_d + c_w + c_v + c_y$, $\boldsymbol{\mu}^2_{\nu\tau}[i](i \in \mathbb{Z}^+_\zeta)$ for the last $\rho + 1$ to $\rho + \zeta$ rows with $\zeta = 2p(\overline{\tau} - t_s + 1)$. Finally, the KKT conditions are given as follows:

$$0 = R^\top_{\nu,\tau}[:, m]\,\text{vec}\{\boldsymbol{\mu}^1_{\nu\tau}, \boldsymbol{\mu}^2_{\nu\tau}\}, \forall m \in \mathbb{Z}^+_\xi, 0 = \mathbb{1}^\top\boldsymbol{\mu}^2_{\nu\tau}, \qquad (24a)$$

$$0 \leq \boldsymbol{\mu}^1_{\nu\tau},\ 0 \leq \boldsymbol{\mu}^2_{\nu\tau}, \qquad (24b)$$

$$0 = \boldsymbol{\mu}^1_{\nu\tau}[i](R^\top_{\nu,\tau}[i,:]\bar{x}_{\nu,\overline{\tau}} + S_{\nu,\tau}[i,:]u_{\overline{\tau}-1} - r_{\nu,\tau}[i]), \forall i \in \mathbb{Z}^+_\rho, \qquad (24c)$$

$$0 = \boldsymbol{\mu}^1_{\nu\tau}[i](R^\top_{\nu,\tau}[i+\rho,:]\bar{x}_{\nu,\overline{\tau}} - r_{\nu,\tau}[i+\rho] + S_{\nu,\tau}[i+\rho,:]u_{\overline{\tau}-1} - \delta_{\nu,\tau}), \forall i \in \mathbb{Z}^+_\zeta, \qquad (24d)$$

where (24a) is the stationarity condition, (24b) is the dual feasibility, and (24c), (24d) serve as complementary slackness that can either be described as *SOS-1* constraints or be reformulated using *big-M* method. □

Theorem 1 solves Problem 1 and the MILP can be solved efficiently using off-the-shelf solvers, e.g., Gurobi [16].

B. Construction of IMI Tree

First, we enable the trace concatenation operation using the operator $\oplus$. Given $\omega_{\overline{\alpha}}(\mathbb{V}_{\underline{\alpha}})$ and $\omega_{\overline{\beta}}(\mathbb{V}_{\underline{\beta}})$ satisfying $\overline{\alpha} + 1 = \underline{\beta}$ and $\omega_{\overline{\alpha}}(\mathbb{V}_{\underline{\alpha}})[\overline{\alpha}] \supseteq \mathbb{V}_{\underline{\beta}}$, the concatenated trace $\omega_{\overline{\beta}}(\mathbb{V}_{\underline{\alpha}}) := \omega_{\overline{\alpha}}(\mathbb{V}_{\underline{\alpha}}) \oplus \omega_{\overline{\beta}}(\mathbb{V}_{\underline{\beta}})$ with its first $\overline{\alpha} - \underline{\alpha} + 1$ elements identical to $\omega_{\overline{\alpha}}(\mathbb{V}_{\underline{\alpha}})$ and the remaining the same as $\omega_{\overline{\beta}}(\mathbb{V}_{\underline{\beta}})$.

Proposition 1 (Partition)**.** *Given any trace $\omega_{\overline{t}}(\mathbb{V}_{\underline{t}})$, it can be partitioned as $\omega_{\overline{t}}(\mathbb{V}_{\underline{t}}) = \omega_{\alpha-1}(\mathbb{V}_{\underline{t}}) \oplus \omega^*_{\overline{t}}(\mathbb{V}_\alpha)$ $\alpha \in \mathbb{Z}^{\underline{t}}_{\overline{t}}$ (i.e., a general trace followed by an identical trace).*

Proof. This directly follows from Definition 4. □

Definition 7 (Exact Partition)**.** *An exact partition $\omega_{\overline{t}}(\mathbb{V}_{\underline{t}}) = \omega_{\alpha-1}(\mathbb{V}_{\underline{t}})\bar{\oplus}\omega^*_{\overline{t}}(\mathbb{V}_\alpha)$ enforces $\omega_{\alpha-1}(\mathbb{V}_{\underline{t}})[\alpha-1] \supset \mathbb{V}_\alpha$, where $\bar{\oplus}$ is particularly used for exact partition.*

Proposition 2. *The exact partition of any trace is unique.*

Proof. Assume two exact partitions exist, i.e., $\omega_{\bar{t}}(\mathbb{V}_{\underline{t}}) = \omega_{\alpha-1}(\mathbb{V}_{\underline{t}})\bar{\oplus}\omega^*_{\bar{t}}(\mathbb{V}_\alpha) = \omega_{\beta-1}(\mathbb{V}_{\underline{t}})\bar{\oplus}\omega^*_{\bar{t}}(\mathbb{V}_\beta)$, and without loss of generality, let $\alpha < \beta$. $\omega^*_{\bar{t}}(\mathbb{V}_\alpha)$ forces that $\omega_{\bar{t}}(\mathbb{V}_{\underline{t}})[\beta - 1] = \mathbb{V}_\beta$, which violates the subset relation enforced by the definition of exact partition at β. □

Proposition 3 (Complete Exact Partition)**.** *Any trace $\omega_{\bar{t}}(\mathbb{V}_{\underline{t}})$ can be partitioned as a concatenation of multiple identical traces, i.e., $\omega_{\bar{t}}(\mathbb{V}_{\underline{t}}) = \bar{\bigoplus}_{\pi=1}^{F}\omega^*_{\overline{t_\pi}}(\mathbb{V}_{\underline{t_\pi}})$ with $\mathbb{V}_{\underline{t_\pi}} \supset \mathbb{V}_{\underline{t_{\pi+1}}}$, and this complete exact partition is unique.*

Proof. This directly follows from Propositions 1 and 2. □

Definition 8 (End Replication)**.** *Given any trace $\omega_{\bar{t}}(\mathbb{V}_{\underline{t}})$, we define the end replication operation formally given as $\mathcal{ER}(\omega_{\bar{t}}(\mathbb{V}_{\underline{t}}), m) := \omega_{\bar{t}}(\mathbb{V}_{\underline{t}})\bar{\oplus}\omega^*_{\bar{t}+m}(\omega_{\bar{t}}(\mathbb{V}_{\underline{t}})[\bar{t}])$.*

The $\mathcal{ER}$ operation generates a new trace by replicating the last entry of a trace multiple times and is used in Algorithm 1 to construct the IMI tree (cf. Problem 4). For each trace in $\mathcal{T}^0_{T-1}(\mathbb{Z}^+_N)$, first determine its complete exact partition. Next, starting with $\pi = 1$, concatenate the first π identical traces to obtain a length t trace, then extend its length to T with end replication and design separating inputs by TAMD. Lastly, save the first t inputs as fixed values for the next iteration.

Algorithm 1: Construction of IMI Tree

Data: $\mathcal{G}_i$, (3)-(9), $\mathcal{T}^0_{T-1}(\mathbb{Z}^+_N)$
Result: $\mathcal{TR}(\mathbb{Z}^+_N)$
for *Each trace $\omega_{T-1}(\mathbb{V}_0 = \mathbb{Z}^+_N)$ in $\mathcal{T}^0_{T-1}(\mathbb{Z}^+_N)$* **do**
  Obtain $\omega_{T-1}(\mathbb{Z}^+_N) = \bar{\bigoplus}_{\pi=1}^{F}\omega^*_{\overline{t_\pi}}(\mathbb{V}_{\underline{t_\pi}})$;
  Initialization: $\pi \leftarrow 1$; $t \leftarrow \underline{t_1}$; $u^*_0 = \emptyset$;
  while $i \le q$ **do**
    $\omega = \mathcal{ER}(\bar{\bigoplus}_{k=1}^{\pi}\omega^*_{\overline{t_k}}(\mathbb{V}_{\underline{t_k}}), T - 1 - \overline{t_k})$;
    Design control u_{T-1} for ω by TAMD;
    $\pi \leftarrow \pi + 1$;
    $t \leftarrow t \leftarrow \underline{t_\pi}$;
    $u^*_{t-1} = u_{T-1}[0 : t-1]$;
  end
end

C. Model Invalidation

The MI problem can be formulated as a feasibility check of an LP which is formally stated as follows:

Theorem 2. *Given model $\mathcal{G}_i$ and the input-output sequence $\{\tilde{u}(k), \tilde{z}(k+1)\}_{k=0}^{t-1}$, the model invalidation problem given in Problem 2 is equivalent to checking the feasibility of the following problem:*

$$\begin{aligned}
&\textit{Find} \quad \bar{x}_{i,t} \\
&\textit{s.t.} \quad (\bar{P}^t_{\bar{\boldsymbol{x}},i}\Phi^t_i)\bar{x}_{i,t} \le \bar{p}^t_{\bar{\boldsymbol{x}},i} - \bar{P}^t_{\bar{\boldsymbol{x}},i}\bar{f}^t_i - (\bar{P}^t_{\bar{\boldsymbol{x}},i}\Omega^t_{ui})\tilde{u}_{t-1}, && \text{(25a)}\\
&\qquad \Psi^t_i\bar{x}_{i,t} = -\bar{E}^t_{ui}\tilde{u}_{t-1} - \bar{\theta}^t_i + \tilde{z}^+_{i,t}, && \text{(25b)}\\
&\qquad H^t_{\bar{x},i}\bar{x}_{i,t} \le h^t_{\bar{x},i}, && \text{(25c)}
\end{aligned}$$

where $\bar{P}^t_{\bar{\boldsymbol{x}},i} = \mathrm{diag}_t\{\mathrm{diag}\{P_{x,i}, P_{y,i}\}\}$ *and* $\bar{p}^t_{\bar{\boldsymbol{x}},i} = \mathrm{vec}_t\{\mathrm{vec}\{p_{x,i}, p_{y,i}\}\}$.

Proof. First, the constraints (1), (2) are expressed as the concatenated equations (14a) and (14d). Then, it is straightforward to see that (25a) is a concatenated form of (14a), (6) and (7) associated with $\bar{x}_{i,t}$, and (25b) is equivalent to (14d). Lastly, (25c) is a combination of (3), (5), (8) and (9). □

Theorem 2 solves Problem 2 and the computational cost of the resulting feasibility check of an LP is relatively low. which renders its online applicability.

D. Integrated Model Identification

Given the IMI tree computed recursively using TAMD and the online-solvable MI technique, we provide our novel algorithm for real-time model identification as described in Algorithm 2, which can be viewed as a direct implementation of Problem 3 (see also Remarks 3 and 4). Further, given the IMI tree $\mathcal{TR}(\mathbb{Z}^+_N)$, the extracted inputs corresponding to a trace $\omega_t(\mathbb{Z}^+_N)$ is defined as a mapping $\mathcal{C}(\cdot)$. The algorithm terminates once the index set $\mathbb{V}_t$ has only one element which is the index of the identified model.

Algorithm 2: IMI Implementation

Data: $\mathcal{G}_i$, (3)-(9), $\mathcal{TR}(\mathbb{Z}^+_N)$, $\bar{\boldsymbol{x}}(0)$
Result: The identified Model Index i^*
Initialization: $t \leftarrow 0$; $\mathbb{V}_0 \leftarrow \mathbb{Z}^+_N$; $\omega_0[0] \leftarrow \mathbb{Z}^+_N$;
while $|\mathbb{V}_t| \ge 2$ *and* $t \le T$ **do**
  Go to branch $\mathcal{BR}^0_{T-1}(\omega_t(\mathbb{Z}^+_N))$;
  $\tilde{u}(t) \leftarrow \mathcal{C}(\omega_t(\mathbb{Z}^+_N)[t])$;
  Compute $\tilde{z}(t+1)$ as in (1), (2) with $w(t)$, $v(t+1)$;
  Update $\{\tilde{u}(k), \tilde{z}(k+1)\}_{k=0}^{t}$;
  Compute $\mathbb{V}_{t+1}$ by MI using $\{\tilde{u}(k), \tilde{z}(k+1)\}_{k=0}^{t}$;
  $\omega_{t+1} \leftarrow \omega_t \oplus \mathbb{V}_{t+1}$;
  $t \leftarrow t + 1$;
end
$i^* \leftarrow$ the only element of $\mathbb{V}_t$

Further, computational complexity of TAMD and MI in terms of the number of continuous variables (CV), integer variables (IV) and constraints are summarized in TABLE I.

TABLE I: Complexity of TAMD (Big-M Formulation) and MI

	TAMD	MI
No. of CV	$\mathcal{O}((c_xN_t + 2I_t)c_sT^2)$	$n + tm_s$
No. of IV	$\mathcal{O}(c_sI_tT^2)$	0
No. of constraints	$\mathcal{O}((c_xc_sN_t + (5c_s + m_s)I_t)T^2)$	$c_0 + (c_s + c_x - c_y + p)t$

V. Simulation Example

The integrated model identification method is applied to a highway lane-changing scenario in [3] to identify the intention of other road participants, where the input of the ego vehicle is designed to distinguish the intentions of the human-driven vehicle. The equations of motion are:

$$\begin{aligned}
x_e(k+1) &= x_e(k) + v_{x,e}(k)\delta t,\\
v_{x,e}(k+1) &= v_{x,e}(k) + u_{x,e}(k)\delta t + w_{x,e}(k)\delta t,\\
y_e(k+1) &= y_e(k) + v_{y,e}(k)\delta t + w_{y,e}(k)\delta t,\\
x_o(k+1) &= x_o(k) + v_{x,o}(k)\delta t,\\
v_{x,o}(k+1) &= v_{x,o}(k) + d(k)\delta t + w_{x,o}(k)\delta t,
\end{aligned}$$

where $x_e(v_{x,e})$ and $x_o(v_{x,o})$ are the longitudinal position (velocity) of the ego car and the other car, respectively. In the lateral direction, only the position (velocity) of the ego car, denoted as y_e $(v_{y,e})$, is considered. $u_{x,e}$ and d represent the longitudinal acceleration input for the ego car and the other car, respectively. Here, $u = [u_{x,e}, v_{y,e}]$ is the separating control and d is the uncontrolled input reflecting the other car's intent. Both vehicles are affected by noise w. In addition, the system's output is the longitudinal velocity of the other car given as $z(k) = v_{x,o}(k) + v(k)$ with output noise $v(k)$. Both cars are close to their center lane initially.

We have 3 models corresponding to the other car's 3 intentions (i.e., Inattentive (I), Cautious (C) and Malicious (M)). Their detailed description can be found in [3].

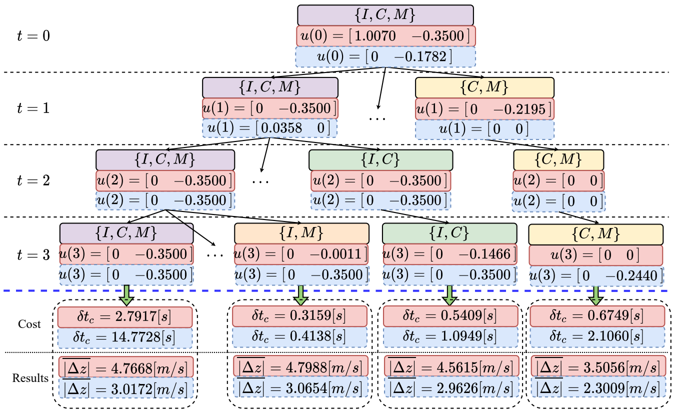

Fig. 1: IMI Tree (TAMD: red; AMD: blue)

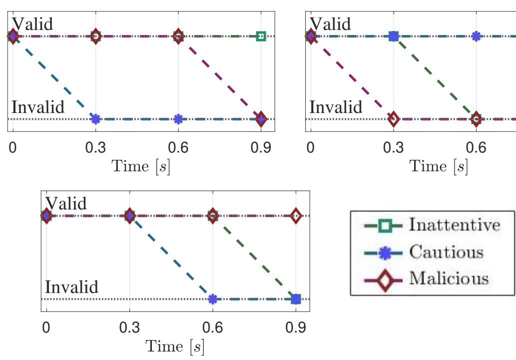

Fig. 2: IMI results: Models I (top left), C (top right), M (bottom).

In the simulation, the initial position of the ego car is 0 m, while constraints on initial position of the other car, input constraints, state constraints and noise bounds are set as in [3]. Time horizon $T = 4$ with the sampling time $\Delta t = 0.3$s. For TAMD, we consider the complete partition (i.e., $\tau \in \mathbb{Z}_4^+$, $\underline{\tau} = \overline{\tau}$) and the desired separation is chosen to be $\epsilon_\tau = 0.25$, the weights $\lambda_\tau = 0.1 + 0.05\tau$, and $J(\cdot) = ||\cdot||_1$. Both TAMD and online MI are solved using Gurobi 9.1.2 [16].

The IMI tree, which specifically presents 4 representative traces in terms of inputs $u(t)$, computational cost δt_c and discrimination performance $\overline{|\Delta z|}$, is shown in Fig. 1. δt_c is the time cost of solving the optimization and $\overline{|\Delta z|} := \frac{1}{3KT}\sum_{k=1}^{K}\sum_{t=1}^{T}\sum_{i\neq j}|z_i(t) - z_j(t)|$ is the average output difference over K runs ($K = 100$), all time instants $t \in \mathbb{Z}_T^+$ and all pairs. Results using TAMD and the traditional AMD [3] are shown with red and blue undertones, respectively. From Fig. 1, we observe that TAMD discriminates the models more and requires significantly less computational cost (albeit with increased $J(u_{T-1})$) than AMD in [3]. The online MI is a linear program without integer variables and its computational cost is around 0.03s for all tests, which demonstrates the online applicability of the IMI algorithm.

The final IMI results using TAMD are shown in Fig. 2. For all 3 intentions, the IMI algorithm with the inputs designed by TAMD successfully identifies the correct intention.

VI. Conclusion

In this paper, we proposed a novel passive-active model identification algorithm that combines TAMD and MI techniques, where TAMD guarantees improved discrimination performance in terms of more design flexibility and potentially reduced computational cost. A novel IMI tree architecture and an algorithm for its construction are also presented, which assists the online implementation of IMI. Simulations of an autonomous driving with intention identification example in a lane-changing scenario demonstrates the applicability and effectiveness of the proposed algorithms.

References

[1] S. Z. Yong, M. Zhu, and E. Frazzoli. Generalized innovation and inference algorithms for hidden mode switched linear stochastic systems with unknown inputs. In *IEEE CDC*, pages 3388–3394, 2014.

[2] A. Abdo, S. X. Ding, J. Saijai, and W. Damlakhi. Fault detection for switched systems based on a deterministic method. In *IEEE Conference on Decision and Control (CDC)*, pages 568–573, 2012.

[3] Y. Ding, F. Harirchi, S. Z. Yong, E. Jacobsen, and N. Ozay. Optimal input design for affine model discrimination with applications in intention-aware vehicles. In *ACM/IEEE International Conference on Cyber-Physical Systems (ICCPS)*, pages 5161–5167, 2018.

[4] F. Harirchi and N. Ozay. Guaranteed model-based fault detection in cyber–physical systems: A model invalidation approach. *Automatica*, 93:476–488, 2018.

[5] P. Rumschinski, S. Borchers, S. Bosio, R. Weismantel, and R. Findeisen. Set-base dynamical parameter estimation and model invalidation for biochemical reaction networks. *BMC systems biology*, 4(1):69, 2010.

[6] H. Lou and P. Si. The distinguishability of linear control systems. *Nonlinear Analysis: Hybrid Systems*, 3(1):21–38, 2009.

[7] A. Halder and R. Bhattacharya. Model validation: A probabilistic formulation. In *IEEE Conference on Decision and Control and European Control Conference*, pages 1692–1697, 2011.

[8] P. Rosa and C. Silvestre. On the distinguishability of discrete linear time-invariant dynamic systems. In *IEEE CDC-ECC*, pages 3356–3361, 2011.

[9] F. Harirchi, S.Z. Yong, E. Jacobsen, and N. Ozay. Active model discrimination with applications to fraud detection in smart buildings. In *IFAC World Congress, Toulouse, France*, 2017.

[10] Q. Shen and S.Z. Yong. Active model discrimination using partition-based output feedback input design. In *2020 European Control Conference (ECC)*, pages 712–717. IEEE, 2020.

[11] K. Singh, Y. Ding, N. Ozay, and S.Z. Yong. Input design for nonlinear model discrimination via affine abstraction. *IFAC-PapersOnLine*, 51(16):175–180, 2018.

[12] G. R. Marseglia and D. M. Raimondo. Active fault diagnosis: A multi-parametric approach. *Automatica*, 79:223–230, May 2017.

[13] R. Niu, Q. Shen, and S. Z. Yong. Partition-based parametric active model discrimination with applications to driver intention estimation. In *European Control Conference (ECC)*, pages 3880–3885, 2019.

[14] D. M. Raimondo, G. R. Marseglia, R. D. Braatz, and J. K. Scott. Closed-loop input design for guaranteed fault diagnosis using set-valued observers. *Automatica*, 74:107–117, Dec. 2016.

[15] F. Harirchi and N. Ozay. Model invalidation for switched affine systems with applications to fault and anomaly detection. *IFAC-PapersOnLine*, 48(27):260–266, 2015.

[16] Gurobi Optimization, Inc. Gurobi optimizer reference manual, 2021.

Appendix

In this appendix, we provide definitions of matrices and vectors that were previously omitted to improve readability. In the following, $\dagger = \{u, d, w\}$, $\diamond = \{x, y\}$.

$$\overline{M}_i^t = \begin{bmatrix} A_i \\ A_i^2 \\ \vdots \\ A_i^t \end{bmatrix}, \overline{A}_i^t = \begin{bmatrix} \mathbb{I} & 0 & \cdots & 0 \\ A_i & \mathbb{I} & \cdots & 0 \\ \vdots & & \ddots & \\ A_i^{t-1} & A_i^{t-2} & \cdots & \mathbb{I} \end{bmatrix},$$

$$\overline{A}_i^t \boxtimes B := \begin{bmatrix} B & 0 & \cdots & 0 \\ A_i B & B & \cdots & 0 \\ \vdots & \vdots & \ddots & \\ A_i^{t-1}B & A_i^{t-2}B & \cdots & B \end{bmatrix}, M^t := \mathbb{I}_t \otimes M,$$

$$A_i = \begin{bmatrix} A_{x,i} \\ A_{y,i} \end{bmatrix}, B_{\dagger,i} = \begin{bmatrix} B_{x\dagger,i} \\ B_{y\dagger,i} \end{bmatrix}, f_i = \begin{bmatrix} f_{x,i} \\ f_{y,i} \end{bmatrix},$$

$$\Gamma_{\dagger i}^t = \overline{A}_i^t \boxtimes B_{\dagger,i},\ \bar{f}_i^t = \overline{A}_i^t(\mathbb{1}_t \otimes f_i),\ \bar{f}_i^{\diamond,t} = A_{\diamond,i}^t \bar{f}_i^t + \mathbb{1}_t \otimes f_{\diamond,i},$$
$$M_i^{\diamond,t} = A_{x,i}^t \overline{M}_i^t,\ \Gamma_{\dagger i}^{\diamond,t} = A_{\diamond,i}^t \Gamma_{\dagger i}^t + B_{\diamond\dagger,i}^t,\ \bar{C}_i^t = C_i^t \overline{A}_i^t,$$
$$\bar{D}_{ui}^t = C_i^t \Gamma_{ui}^t,\ \bar{D}_{di}^t = C_i^t \Gamma_{di}^t,\ \bar{D}_{wi}^t = C_i^t \Gamma_{wi}^t,$$
$$\bar{D}_{vi}^t = D_{v,i}^t,\ \bar{\theta}_i^t = C_i^t \bar{f}_i^t + \mathbb{1}_t \otimes g_i.$$